

What does the crystallography of stones tell us about their formation?

Peter Rez¹

Received: 31 August 2016 / Accepted: 22 November 2016 / Published online: 29 November 2016
© Springer-Verlag Berlin Heidelberg 2016

Abstract The mineral phase makes up most of the mass of a kidney stone. Minerals all come in the form of crystals that are regular arrangements of atoms or molecular groupings at the atomic scale, bounded macroscopically by well-defined crystal faces. Pathologic nephroliths are a polycrystalline aggregate of submicron crystals. Organic macromolecules clearly have an important role in either promoting or preventing aggregation and in altering the morphology of individual submicron crystals by influencing the surface energies of different faces. Crystals, similar in morphology to those grown in solution, are often found for calcium oxalate dihydrate, brushite, cystine and struvite. This is not the case for calcium oxalate monohydrate and hydroxyapatite, two of the most common constituents of stones.

Keywords Urolithiasis · Crystal structure · SEM · AFM

Introduction

Kidney stones are an example of pathological biomineralization; they clearly have no beneficial effect. Both pathological and normal biominerals have both solid mineral phases and organic phases. For kidney stones, the weight fraction for the organic matrix is on average 3% for calcium containing or uric acid stones and 9% for cystine stones [5, 35]. Given that most of the mass of a stone is the solid or mineral phase the mechanisms by which it

nucleates and grows are of fundamental importance. Even though the organic matrix is a minor component, the role of organic macromolecules, such as proteins or lipids is an important question for both normal and pathological biomineralization.

The most prevalent kidney stones are those composed of calcium oxalate, usually as its monohydrate polymorph, though it can be present as the dihydrate. The trihydrate form has not been detected in kidney stones. The mineral that makes up Randall's plaques calcium hydroxyapatite (a phosphate) is also seen in kidney stones. Other phosphates, such as octacalcium phosphate and brushite are also stone constituents, and mixed phosphate oxalate stones are quite common. In acidic urine (low pH), it is possible to form stones composed of uric acid and related compounds such as monosodium urate. A metabolic disorder leading to cystinuria can result in cystine stones, and infection can lead to stones formed from struvite, magnesium ammonium phosphate. Summaries of the prevalence of different minerals in stones have been given by Prien and Prien [49] and Herring [28].

From a materials science perspective the micro and nano structure gives vital information on how any material is formed. This should also be true for biominerals. Minerals, including the solid phases in biominerals, are all crystals. Macroscopically, a crystal is a solid with well-defined facets. At the atomic level it is a regular arrangement of atoms or molecular groups arranged according to well-defined symmetries. This gives a perfect lattice of points extending throughout the crystal. The fundamental repeating unit of lattice points in identical environments is called the unit cell. It is specified in terms of its sides and angles between them (see Fig. 1a). Rotational symmetry defines the crystal system. It can be shown that for an infinite repeating lattice of points only 1-, 2-, 3-, 4-, and 6-fold rotations are allowed. A summary of the crystal systems is given in Table 1.

✉ Peter Rez
Peter.Rez@asu.edu

¹ Department of Physics, Arizona State University, Tempe, AZ 85287-1504, USA

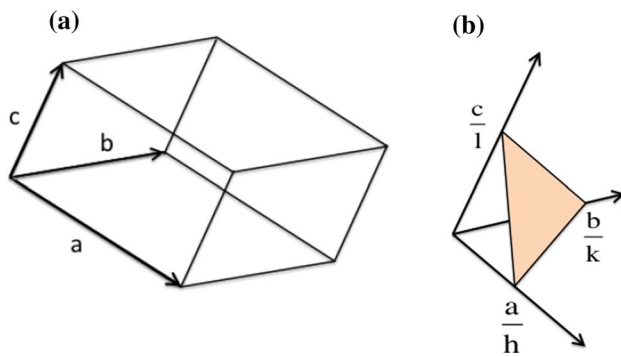


Fig. 1 **a** The unit cell in a crystal **b** planes are specified by the intercepts of the plane with the unit cell sides

The table shows a steady progression from lesser to greater symmetry. Adding other symmetries, such as mirror reflections, or twofold rotations perpendicular to the main rotation axis, gives the 32 point groups. When translation symmetries are added, 230 space groups are generated. Traditionally, information on space groups came from the International Tables for Crystallography [25], but these days it is easier to use a program such as CrystalMaker® (<http://www.crystallmaker.com>). Atom positions in the crystal structure are specified relative to the sides of the unit cell.

The crystal facets are specified in terms of plane indices. A plane is drawn within the first unit cell. The plane cuts the unit cell sides at certain positions, specified by the fraction of the cell side. The plane indices (h, k, l) are the inverse of these fractions (see Fig. 1b). The plane indices also define potential crystal surfaces. Wulff [79] gave a simple construction to determine the shape of the macroscopic crystal. Each of the facets specified by a plane index (h, k, l) has a surface energy γ_{hkl} . The aim is to minimize the total surface energy. Lines are drawn along the (hkl) directions with length proportional to the surface energy γ . At the end of each line a perpendicular line is drawn. The boundary sketched out by these perpendicular lines is the macroscopic shape of the crystal (see Fig. 2). It is easy to see that surfaces with a high surface energy are smaller than those with a lower surface energy.

So far we have only considered perfect infinite crystal lattices. In practice, there are also defects or other imperfections and these might be significant for the biominerals making up kidney stones.

Crystal structures of common stone constituents

When grown in solution, or found as naturally occurring minerals, the materials making up kidney stones show characteristic shapes defined by the most prominent crystal facets. Lonsdale [40] and Frincu [20], in their study of epitaxial relationships, give a comprehensive list of crystallographic information, such as space group, unit cell parameters and prominent crystal facets. For convenience, we repeat it here as Table 2 divided into oxalates, phosphates, urates and cystine.

For COM we are using the unit cell of Tazzoli and Domeneghetti [73].

Some authors use the unit cell of Deganello [11].

$\mathbf{a}_{\text{Deg}} = -(\mathbf{a}_{\text{Tazz}} + \mathbf{c}_{\text{Tazz}})$, $\mathbf{c}_{\text{Deg}} = \mathbf{a}_{\text{Tazz}}$. A listing giving equivalent plane indices for both choices of unit cell is given by Millan [46].

Factors affecting crystal growth

For urolithiasis, the first question is whether these crystal forms are actually present in kidney stones. The characteristic bipyramids formed by the {101} faces of calcium oxalate dihydrate are easily recognized [34, 55]. In COM stones polarized light microscopy and SEM reveal concentric rings and radial striations [45, 47, 64, 65]. Structures recognizable as COM crystals with the expected facets (see Fig. 3a) have rarely been seen [8, 63, 77], even though the stones have been unambiguously identified as COM by powder X-ray diffraction. On the basis of polarized microscopy Al Atar et al. [1] proposed that crystals with the expected (100) faces, elongated in the [001] direction, are stacked together as domains up to 50 μ across, consistent with the stacks observed in SEM. There is a similar problem for some of the phosphates. Khan et al. [32, 34] and Spector et al. [69] show a spherulitic microstructure that does not resemble the expected cuboidal apatite shape.

Table 1 The crystal systems

Crystal symmetry	Fundamental rotational symmetry	Unit cell sides	Unit cell angles
Triclinic	1-fold	Sides unequal	Angles unequal
Monoclinic	2-fold	Sides unequal	$\alpha = \gamma = 90^\circ$
Orthorhombic	Three orthogonal 2-folds	Sides unequal	$\alpha = \beta = \gamma = 90^\circ$
Tetragonal	4-fold	$a = b$	$\alpha = \beta = 90, \gamma = 90^\circ$
Hexagonal	6-fold	$a = b$	$\alpha = \beta = 90, \gamma = 120^\circ$
Rhombohedral	3-fold	$a = b = c$	$\alpha = \beta = \gamma$
Cubic	Orthogonal 3-folds	$a = b = c$	$\alpha = \beta = \gamma = 90^\circ$

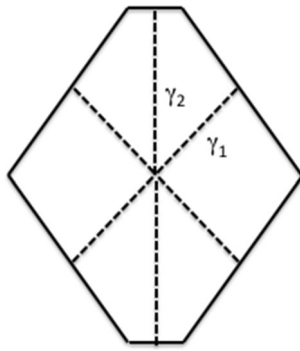


Fig. 2 The Wulff construction. Note that the smaller face has a higher surface energy

It is only with brushite [34, 55], struvite and cystine that crystals with the expected facets have been unambiguously seen in the stones themselves.

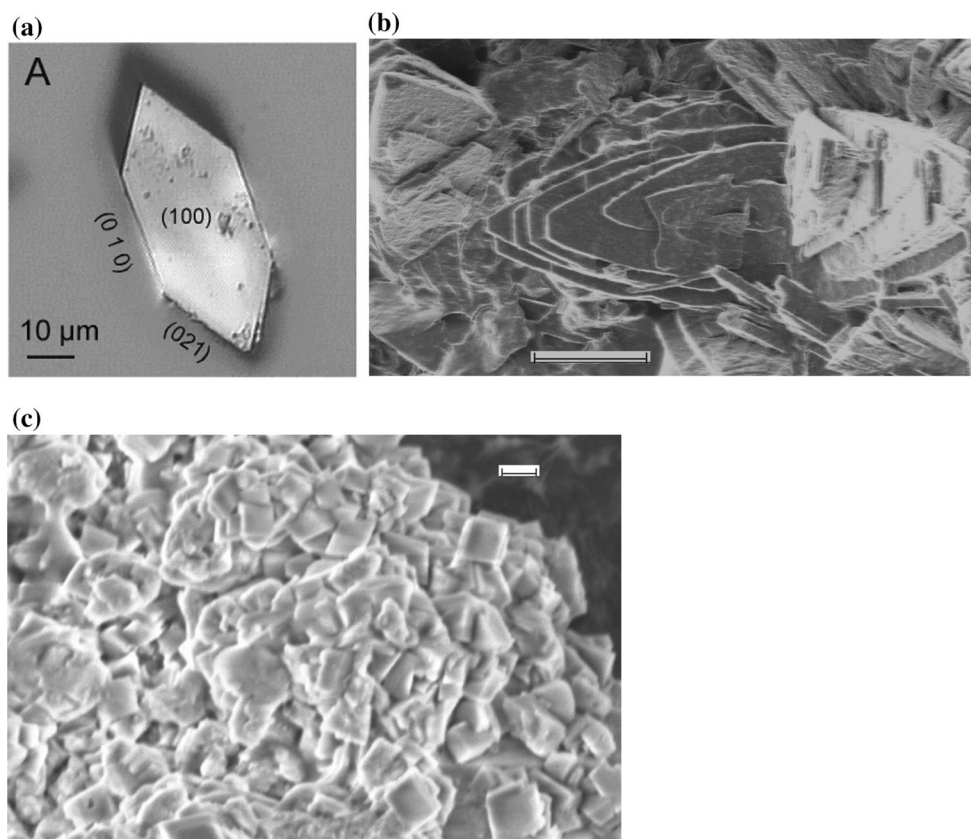
It is widely believed that urinary macromolecules can inhibit the growth of crystals. It would therefore not be surprising that the shape of a crystal that has grown in urine (or possibly originated in some intracellular space) is strongly influenced by the organic macromolecules that are inevitably present. The surface energies will change and organic molecules might prevent the addition of new ions from solution by blocking favorable step sites. This has been graphically demonstrated in the liquid AFM studies of Qiu, who showed how citrate binds at the [001] steps

Table 2 Summary of crystallographic parameters for the most common urinary stone constituents (from Lonsdale [40] and Frincu [20])

Oxalates	Calcium oxalate monohydrate (COM) $\text{Ca}(\text{C}_2\text{O}_4) \cdot \text{H}_2\text{O}$ #		Calcium oxalate dihydrate (COD) $\text{Ca}(\text{C}_2\text{O}_4) \cdot 2\text{H}_2\text{O}$
System	Monoclinic		Tetragonal
Space group	$P2_1/c$		$I4/m$
Lattice	$a = 6.29, b = 14.583, c = 10.116$ $\beta = 109.46$		$a = b = 12.37, c = 7.357$
Planes	$(100) (011) (010) (021) (0\bar{2}1) (12\bar{1}) (1\bar{2}\bar{1})$		$(101) (100) (010)$
Phosphates	Hydroxyapatite $\text{Ca}_5(\text{PO}_4)_3\text{OH}$	Brushite $\text{CaHPO}_4 \cdot 2\text{H}_2\text{O}$	Octacalcium phosphate $\text{Ca}_8\text{H}_2(\text{PO}_4)_6 \cdot 5\text{H}_2\text{O}$
System	Hexagonal	Monoclinic	Triclinic
Space group	$P6_3/m$	$I2/a$	$P1$
Lattice	$a = 9.418, c = 6.875$	$a = 5.88, b = 15.15, c = 6.37$ $\beta = 117.46^\circ$	$a = 19.87, b = 9.63, c = 6.88$ $\alpha = 89.3^\circ, \beta = 92.2^\circ, \gamma = 108.9^\circ$
Planes	$(0001) (10\bar{1}0) (11\bar{2}0) (11\bar{2}2)$ $(10\bar{1}1) (1012) (20\bar{2}1)$	$(010) (001) (101) (120) (\bar{1}11) (1\bar{1}0)$	$(100) (010) (001)$
Urates	Uric acid $\text{C}_5\text{H}_4\text{N}_4\text{O}_3$	Uric acid dihydrate $\text{C}_5\text{H}_4\text{N}_4\text{O}_3 \cdot 2\text{H}_2\text{O}$	Monosodium urate $\text{C}_5\text{H}_3\text{N}_4\text{NaO}_3$
System	Monoclinic	Monoclinic	Triclinic
Space group	$P2_1/a$	$P2_1/c$	$P\bar{1}$
Lattice	$a = 14.46, b = 7.403, c = 6.281$ $\beta = 65.1^\circ$	$a = 7.237, b = 6.363, c = 17.449$ $\beta = 90.51^\circ$	$a = 10.888, b = 9.534, c = 3.567$ $\alpha = 95.06^\circ, \beta = 99.47^\circ, \gamma = 97.17^\circ$
Planes	$(100) (210) (201) (001)$	$(001) (102) (011)$	$(100) (001) (010)(1\bar{1}0)$
Struvite and cystine	Struvite $\text{MgNH}_4\text{PO}_4 \cdot 6\text{H}_2\text{O}$	Cystine $(\text{C}_3\text{O}_2\text{NH}_5\text{S})_2$	
System	Orthorhombic	Hexagonal	
Space group	$P2_1mn$	$P6_122$	
Lattice	$a = 6.6955, b = 6.142, c = 11.218$	$a = 5.6422, c = 5.6275$	
Planes	$(011) (102) (100) (001)$	$(001) (11\bar{2}0)$	

Unit cell lengths are given in Angstroms

Fig. 3 **a** COM crystal precipitated from solution from Guo et al. [24]. **b** SEM from fracture surface of COM stone showing plates with rounded edges. Bar is 10 μ . Note the similarity to Fig. 4b of Daudon et al. [8]. **c** SEM of sonicated COM stone showing submicron crystals. Bar is 200 nm



on the (100) surface of COM and how osteopontin slowed the growth of the (010) facets [50, 51]. These studies were extended to cystine by Mandal and Ward [42]. Some of the results showing curved faces might explain the morphology observed by Sandersius et al. [63], also shown as Fig. 3b.

Given that powder diffraction of stones shows sharp peaks characteristic of a polycrystalline, not an amorphous material, the size of the individual crystallites is still an open question. High-resolution scanning electron microscopy and AFM have both indicated that any crystallites are submicron in size [12, 63]. Analysis of peak widths from synchrotron diffraction has been used to measure size distributions and internal strains in crystals precipitated from urine [19]. X-ray diffraction peak profiles were also used to confirm SEM size estimates of crystallites in stones [21]. Considerations of the ratio of organic matrix to mineral phase also suggest that the mineral crystallites are submicron in size. According to Sandersius [63], if the matrix completely surrounds the mineral crystallites as a monolayer of the organic macromolecule then the crystallite size varies from 0.3 μ for a monolayer of 10 kD protein to 0.47 μ for a monolayer of 30 kD protein or phospholipid. The crystals could be as large as 0.7 μ for a monolayer of 100 kD protein. If the crystals are in the form of slabs the relevant dimension is the slab thickness. It varies from 53 nm for a small 10 kD protein to 120 nm for a large 100

kD protein. The plates shown in Fig. 3b are 10 μ across and are therefore too large to be the fundamental single crystal units. When COM stones were sonicated and broken apart submicron structures plausibly resembling the expected morphology of COM are visible as shown in Fig. 3c.

However, it is still possible that organic macromolecules are also included inside the mineral crystalline phases. This has been demonstrated experimentally with agarose in calcium carbonate [38], where the inclusions have been mapped at atomic resolution and with fluorescent dyes in uric acid [68]. Ryall's group has shown that various proteins or fragments such as prothrombin fragment 1 [70, 71] are incorporated in COM and COD precipitated from filtered urine. She has argued that these incorporated proteins assist in the break up of submicron crystals when they are attacked by proteases after endocytosis [7, 19, 59–61]. Although small molecules can easily be occluded in growing crystals, it is much harder to incorporate large molecules. That is probably why Tamm Horsfall Glycoprotein, a 100 kD molecule, was not found in crystals grown in urine [62].

Considerations of transit time through the kidney and growth rates also limit the maximum size to a few microns. Finlayson and Reid [18] and Kok and Khan [36] assume COM grows at 1–2 μ min. The growth rate given by Werness et al. [76] is almost an order of magnitude lower, 0.14

μ/min for COM and 0.03 m/min for COD. The transit time through the kidney is 3–4 min, but is only 30–45 s in the collecting duct that has the appropriate supersaturation after water has been removed. That would mean crystallites would range in size from 0.5–1 μ for a growth rate of 1–2 μ/min , and for the lower growth rate of 0.14 μ/min , the size would be limited to 0.07–0.1 μ .

All these arguments suggest that any crystal that form will easily pass through the ureter and will be voided as crystalluria. There have been a number of studies on whether crystalluria is diagnostic for stone disease [9, 54, 75]. In the past these investigations would only have picked up micron sized particles [13], but in a recent paper He [27] explicitly studied nanoparticles. He found that the size distribution in normals was narrower than for stone formers and that the proportion of COD was also higher. This is consistent with some of the earlier studies of crystalluria. In investigations by Rodgers of marathon runners who were all subject to dehydration, a known risk factor for stone disease, the Caucasian stone formers all produced COM aggregates [57, 58], whereas the black non-stone formers produced uniform micron sized COD bipyramids [56]. Interestingly, the dumbbells often associated with COM [34] might easily be confused with COD precipitated with 100–150 $\mu\text{g}/\text{mL}^{-1}$ concentration of polyacrylic acid (PAA) [74]. The increased proportion of COD for non-stone formers would suggest that the formation of COD is a protective normal process, while precipitation of COM is potentially pathological [77]. Further support is provided by the observation that COD is usually found on the outside of mixed COM/COD stones [31]. This raises the question of whether organic macromolecules can control the nucleation of COD v COM in the same way that soluble proteins control the deposition of calcite or aragonite in mollusk shells [2].

So far it has been assumed that the nanometer sized crystals that are the fundamental building blocks for the macroscopic stone all grow according to the classical model. Ion pairs are added one at a time at steps or ledges. However, this seems to be the exception, not the rule, in other areas of biomineralization. Amorphous calcium carbonate (ACC) precursor phases were first found in the sea urchin larval spicule [3]. The hydrated amorphous phase transforms to the crystalline phase through a number of steps [48]. Irregularly shaped perfect crystals can be created through this mechanism. Later it was shown that an amorphous calcium phosphate was involved in the formation of bone [41]. In an excellent recent article, de Yoreo [10] reviews the many possible paths to biomineral crystal formation, including the oriented attachment of crystal nanoparticles. If the paracrystalline model for amorphous calcium carbonate is correct it could be argued that ACC is just an extreme example of crystal particle attachment [52]. The model of crystal particle attachment could explain how the nm sized

crystallites as shown in Fig. 3c assemble to form the larger structures about 10 μ across shown in Fig. 3b.

Is there an amorphous phase that is the initial precursor in oxalate stone formation? The synthesis of amorphous calcium oxalate would suggest that this is a possibility [26, 29]. Given that the formation of calcite from ACC involves dehydration [30] it would seem that COD would be more prevalent than COM if calcium oxalate were initially deposited as a highly hydrated amorphous phase.

By itself the nucleation of submicron crystals does not lead to macroscopic mm or larger stones associated with disease. Although the initial nucleation event is significant, it is the build up of the polycrystalline aggregate that is the key step in the process. Again, organic macromolecules can be of critical importance. Do they hinder or inhibit aggregation or do they act as templates for crystal nucleation and also act as glue for binding small crystals together in polycrystalline arrays?

It is widely believed that macromolecules with carboxylate groups such as Glu and Asp “bind” calcium and proteins rich in Asp and Glu residues were prime candidates for inhibitors of growth and aggregation. Post translation modification of Glu to γ carboxyglutamic acid in proteins such as prothrombin fragment 1 was thought to enhance binding even more [39, 70]. The problem is that in the soluble ordered proteins it is not possible for widely dispersed Glu and Asp residues to make close contact with Ca in crystal surfaces [23]. Stereochemical considerations also limit the ability of both carboxylate groups in Glu residues to bind to surfaces [23]. Of course, there is no reason why basic residues, such as arg and lys might not be attracted to the anions, such as oxalate and phosphate in crystal surfaces. Sheng et al. have used functionalized AFM tips [66, 67] to measure the attractive forces between carboxylate and amidinium groups and (100), (010) and (12 $\bar{1}$) surfaces. The strongest attraction was with the (100) face and the weakest with the (010) face. Attractive forces were measured for both carboxylate and amidinium groups attached to long chains, the forces for carboxylate groups being somewhat higher. Only a disordered or partially ordered protein can make good contact with a mineral surface. It is not surprising that many authors believe that osteopontin is significant in either altering growth or changing aggregation. Using AFM in liquid Qiu showed how osteopontin modulated the (010) faces of COM [50], and demonstrated that it is a potent inhibitor of aggregation. The hypothesis is that the RGD domains interact strongly with mineral surfaces. Grohe et al. used molecular dynamics (MD) to follow how osteopontin might unravel of the (100) surface [22]. However, recent MALDI-TOF of both the urine and stone matrix proteome would suggest that proteins play no special role in stone formation, the main proteins found in stone matrix are those associated with cellular injury [6].

Table 3 Densities of calcium oxalate formula units on various COM and COD surfaces

	a (Å)	b (Å)	Angle (deg)	Area (sq Å)	No of CaOx	Area per Ca or Ox (sq Å)
COM (001)	6.29	7.28	91.5	45.9	1	45.9
COM (010)	6.29	10.3	70	60.9	2	30.5
COM (100)	6.3	7.3	55	37.7	1	37.7
COM (021)	6.26	6.29	105	37.9	1	37.9
COM (10-1)	9.98	7.29	90	72.8	2	36.4
COD (011)	12.37	14.39	90	178	4	44.5
COD (001)	12.37	12.37	90	153	2	38.3
COD (100)	12.37	7.36	90	91	4	45.5

For all the emphasis on proteins as inhibitors (or promoters) of growth or aggregation, this finding would suggest that their presence is adventitious.

Phospholipids potentially have more points of contact with mineral surfaces than ordered proteins. There is considerable evidence of crystal attachment to IMCD (inner medullary collecting duct) cells [43] and RPCT (renal papillary collecting tubule) cells [44, 53] as well as phospholipids on the surface of red blood cells [4]. Controlled growth of COM in the (100) orientation on Langmuir–Blodgett films of phospholipids strongly supports this view [37, 78]. For some time, Khan and colleagues have emphasized the critical role of cellular injury in urolithiasis and the significance of crystal membrane interactions. They showed that phospholipids dominate the matrix of calcific stones and investigated the role of lipid assemblies [33]. A potential problem is that the areal density of phospholipids is greater than the density of Ca ions on most of the COM and COD surfaces (see Table 3). Significant nucleation of COM only occurred when the Langmuir trough pressure reached 20 mN/m and the area per molecule of DPPG (dipalmitoylphosphatidylglycerol) reached 45 Å² [72]. Cell membranes are not uniform layers of a single phospholipid; they are complex arrangements of many different phospholipids with embedded specialized proteins involved in signaling and ion transport. At boundaries it is quite conceivable that there is sufficient compression of headgroups for a good match to oxalate and phosphate mineral surfaces.

Many stones have a mixed composition with two or more different phases. Evan et al. have suggested that oxalate stones originate with Randall's plaques, deposits of apatite in the lower descending loop of Henle. These break through the urothelium and become the nucleus for COM stones encrusting the papillary tip [14, 15, 17]. It was originally suggested by Lonsdale [40] that epitaxy was responsible for overgrowth of one phase over another. A recent analysis by Frincu [20] found many potential epitaxial relations between the many mineral phases that are found in kidney stones. I think these are more of a coincidence, nearly all these minerals are ionic crystals and have similar separation between cations and anions, so it is not

surprising that what appear to be epitaxial relations can be found. It is more likely that overgrowths are facilitated by organic molecules. In fact, Evan et al. found osteopontin and Tamm Horsfall protein [16] between the phosphate and oxalate regions of the composite stone.

Conclusions

Kidney stones are 97% by weight mineral phase and give polycrystalline diffraction patterns. It would therefore be expected that they are aggregates of small crystals. Scanning electron microscopy, AFM and analysis of the width of diffraction peaks suggest that the crystals are submicron in size. Although different phases have been identified by EDX and by their general morphology, the facets of the individual submicron crystals are not easily identified in the fully grown urolith. Radial striations and concentric rings have often been seen in COM stones, and other morphologies have been seen characteristic of different phases. It is still to be determined how much of the organic matrix is intracrystalline and how much fills the space between the submicron crystallites. Any model has to be consistent with the well-known matrix mass fraction. One reason why it is been so hard to identify crystals with shapes corresponding to crystals precipitated from solution is that organic macromolecules alter surface energies of the growing crystal and change the shape, sometimes producing rounded edges. This has been investigated in a controlled way monitoring crystal growth with liquid AFM. Ultimately, the growth of macroscopic kidney stones is controlled by the aggregation of multiple small crystals on those few crystals that have already adhered to the urothelial membrane at a fixed point. Some organic macromolecules play a critical role in facilitating both the adhesion and subsequent agglomeration, though it is also likely that other macromolecules inhibit the process and prevent the small nucleus every growing to macroscopic size and showing clinical symptoms. It is important for research in this area to keep an open mind and not fixate on a particular protein or other macromolecule just because there

is a technology available that makes it easy to detect or because it happens to fit in with a plausible hypothesis.

Acknowledgements I would like to acknowledge financial support from the Rosi and Max Varon visiting professorship while at the Weizmann Institute of Science. Profs Steve Weiner and Lia Addadi made many useful suggestions, and Dr. Eugenia Klein helped in acquisition of SEM micrographs. I'd also like to acknowledge discussions with Prof. Saeed Khan and Dr. Jeff Wesson.

Compliance with ethical standards

Conflict of interest The author has no conflict of interest.

Ethical approval This article does not contain any studies with human participants or animals performed by any of the authors.

References

- Al-Atar U, Bokov AA, Marshall D, Teichman JMH, Gates BD, Ye ZG, Branda NR (2010) Mechanism of calcium oxalate monohydrate kidney stones formation: layered spherulitic growth. *Chem Mater* 22:1318–1329
- Belcher AM, Wu XH, Christensen RJ, Hansma PK, Stucky GD, Morse DE (1996) Control of crystal phase switching and orientation by soluble mollusc shell proteins. *Nature* 381:56–58
- Beniash E, Aizenberg J, Addadi L, Weiner S (1997) Amorphous calcium carbonate transforms into calcite during sea urchin larval spicule growth. *Proc R Soc Lond B* 264:461–465
- Bigelow MW, Wiessner JH, Kleinman JG, Mandel NS (1996) Calcium oxalate-crystal membrane interactions: dependence on membrane lipid composition. *J Urol* 155:1094–1098
- Boyce WH, Garvey FK (1956) The amount and nature of the organic matrix in urinary calculi: a review. *J Urol* 76:213–227
- Canales BK, Anderson L, Higgins L, Ensrud-Bowlin K, Roberts KP, Wu BL, Kim IW, Monga M (2010) Proteome of human calcium kidney stones. *Urology* 76(e1017):e13
- Chauvet MC, Ryall RL (2005) Intracrystalline proteins and calcium oxalate crystal degradation in MDCK II cells. *J Struct Biol* 151:12–17
- Daudon M, Bazin D, Andre G, Jungers P, Cousson A, Chevallier P, Veron E, Matzen G (2009) Examination of whewellite kidney stones by scanning electron microscopy and powder neutron diffraction techniques. *J Appl Crystallogr* 42:109–115
- Daudon M, Hennequin C, Boujelben G, Lacour B, Jungers P (2005) Serial crystalluria determination and the risk of recurrence in calcium stone formers. *Kidney Int* 67:1934–1943
- De Yoreo JJ, Gilbert PUPA, Sommerdijk NAJM, Penn RL, Whitelam S, Joester D, Zhang H, Rimer JD, Navrotsky A, Banfield JF, Wallace AF, Michel FM, Meldrum FC, Colfen H, Dove PM (2015) Crystallization by particle attachment in synthetic, biogenic and geologic environments. *Science* 349:6760
- Deganello S (1981) The structure of whewellite, $\text{CaC}_2\text{O}_4 \cdot \text{H}_2\text{O}$ at 328K. *Acta Crystallogr A* B37:826–829
- Dorian HH, Rez P, Drach GW (1996) Evidence for aggregation in oxalate stone formation: atomic force and low voltage scanning electron microscopy. *J Urol* 156:1833–1837
- Elliot JS, Rabinowitz IN (1980) Calcium oxalate crystalluria: crystal size in urine. *J Urol* 123:324–327
- Evan AP, Lingeman J, Coe FL, Worcester E (2006) Randall's plaque: pathogenesis and role in calcium oxalate nephrolithiasis. *Kidney Int* 69:1313–1318
- Evan AP, Bledsoe SB, Smith SB, Bushinsky DA (2004) Calcium oxalate crystal localization and osteopontin immunostaining in genetic hypercalciuric stone-forming rats. *Kidney Int* 65:154–161
- Evan AP, Coe FL, Lingeman JE, Shao Y, Sommer AJ, Bledsoe SB, Anderson JC, Worcester EM (2007) Mechanism of formation of human calcium oxalate renal stones on Randall's plaque. *Anat Record Adv Integr Anat Evol Biol* 290:1315–1323
- Evan AP, Worcester EM, Coe FL, Williams J, Lingeman JE (2015) Mechanisms of human kidney stone formation Urolithiasis 43:S19–S32
- Finlayson B, Reid F (1978) The expectation of free and fixed particles in stone disease. *Investig Urol* 15:442–448
- Fleming DE, Riessen AV, Chauvet MC, Grover PK, Hunter B, Van Bronswijk W, Ryall RL (2003) Intracrystalline proteins and urolithiasis: a synchrotron X-ray diffraction study of calcium oxalate monohydrate. *J Bone Min Res* 18:1282–1291
- Frincu MC, Fogarty CE, Swift JA (2004) Epitaxial relationships between uric acid crystals and mineral surfaces: a factor in urinary stone formation. *Langmuir* 20:6524–6529
- Ghosh S, Bhattacharya A, Chatterjee P, Mukherjee AK (2014) Structural and microstructural characterization of seven human kidney stones using FTIR spectroscopy, SEM, thermal study and X-ray Rietveld analysis. *Z Kristallogr* 229:451–458
- Grohe B, O'Young J, Ionescu DA, Lajoie G, Rogers KA, Karttunen M, Goldberg HA, Hunter GK (2007) Control of calcium oxalate crystal growth by face specific adsorption of an osteopontin phosphopeptide. *J Am Chem Soc* 129:14946–14951
- Gul A, Rez P (2007) Models for protein binding to calcium oxalate surfaces. *Urol Res* 35:63–71
- Guo S, Ward MD, Wesson JA (2002) Direct visualisation of calcium oxalate monohydrate and crystallization and dissolution with atomic force microscopy and the role of polymeric additives. *Langmuir* 18:4284–4291
- Hahn T (ed) (2005) International tables for crystallography. International Union For Crystallography, Dordrecht
- Hajir M, Graf R, Tremel W (2014) Stable amorphous calcium oxalate: synthesis and potential intermediate in biomineralization. *Chem Commun* 50:6534–6536
- He JY, Deng SP, Ouyang JM (2010) Morphology, particle size distribution, aggregation, and crystal phase of nanocrystallites in the urine of healthy persons and lithogenic patients. *IEEE Trans Nanobiosci* 9:156–163
- Herring LC (1962) Observations on the analysis of ten thousand urinary calculi. *J Urol* 88:545–562
- Ihli J, Wang YW, Cantaert B, Kim YY, Green DC, Bomans PHH, Sommerdijk N, Meldrum FC (2015) Precipitation of amorphous calcium oxalate in aqueous solution. *Chem Mater* 27:3999–4007
- Ihli J, Wong WC, Noel EH, Kim YY, Kulak AN, Christenson HK, Duer MJ, Meldrum FC (2014) Dehydration and crystallization of amorphous calcium carbonate in solution and air. *Nat Commun* 5:3169
- Iwata H, Iio S, Nishio S, Takeuchi M (1992) Architecture of mixed calcium oxalate dihydrate and monohydrate stones. *Scanning Microsc* 6:231–238
- Khan SR (1997) Calcium phosphate/calcium oxalate crystal association in urinary stones: implications for heterogeneous nucleation of calcium oxalate. *J Urol* 157:376–383
- Khan SR, Glenton PA, Backov R, Talham DR (2002) Presence of lipids in urine, crystals and stones: implications for the formation of kidney stones. *Kidney Int* 62:2062–2072
- Khan SR, Hackett RL (1986) Identification of urinary stone and sediment crystals by scanning electron microscopy and X-ray microanalysis. *J Urol* 135:818–826
- King JS, Boyce WH (1957) Amino acid and carbohydrate composition of the mucoprotein matrix in various calculi. *Proc Soc Exp Biol Med* 95:183–187

36. Kok DJ, Khan SR (1994) Calcium oxalate nephrolithiasis, a free or fixed particle disease. *Kidney Int* 46:847–854
37. Letellier JR, Lochlear MJ, Campbell AA, Vogel V (1998) Oriented growth of calcium oxalate monohydrate crystals between phospholipid monolayers. *Biochim Biophys Acta* 1380:31–45
38. Li H, Xin HL, Muller DA, Estroff LA (2009) Visualizing the 3D internal structure of calcite single crystals grown in agarose hydrogel. *Science* 326:1244–1247
39. Lian JB, Prien EL, Glimcher MJ, Gallop PM (1977) The presence of protein bound γ -carboxyglutamic acid in calcium-containing renal calculi. *J Clin Invest* 59:1151–1157
40. Lonsdale K (1968) Epitaxy as a growth factor in urinary calculi and gallstones. *Nature* 217:56–58
41. Mahamid J, Sharir A, Addadi L, Weiner S (2008) Amorphous calcium phosphate is a major component of the forming fin bones of zebrafish: indications for an amorphous precursor phase. *Proc Natl Acad Sci* 105:12748–12753
42. Mandal T, Ward MD (2013) Determination of specific binding interactions at L-cystine crystal surfaces with chemical force microscopy. *J Am Chem Soc* 135:5525–5528
43. Mandel N (1994) Crystal-membrane interaction in kidney stone disease. *J Am Soc Nephrol* 5:S37–S45
44. Mandel N, Riese R (1991) Crystal cell interactions: crystal binding to rat renal papillary tip collecting duct cells in culture. *Am J Kidney Dis* 17:402–406
45. Meyer AS, Finlayson B, DuBois L (1971) Direct observation of urinary stone ultrastructure. *Brit J Urol* 43:154–163
46. Millan A (2001) Crystal growth of whewellite polymorphs: influence of structure distortions on crystal shape. *Cryst Growth Design* 1:245–254
47. Ogbuji LU, Finlayson B (1981) Crystal morphologies in whewellite stones: electron microscopy. *Investig Urol* 19:182–186
48. Politi Y, Metzler R, Abrecht M, Gilbert B, Wilt FH, Sagi I, Addadi L, Weiner S, Gilbert PUPA (2008) Transformation mechanism of amorphous calcium carbonate into calcite in the sea urchin larval spicule. *PNAS* 105:17362–17366
49. Prien EL, Prien EL (1968) Composition and structure of urinary stone. *Am J Med* 45:654–672
50. Qiu SR, Wierzbicki A, Orme CA, Cody AM, Hoyer JR, Nancollas GH, Zepeda S, De Yoreo JJ (2004) Molecular modulation of calcium oxalate crystallization by osteopontin and citrate. *Proc Natl Acad Sci* 101:1811–1815
51. Qiu SR, Wierzbicki A, Salter EA, Zepeda S, Orme CA, Hoyer JR, Nancollas GH, Cody AM, de Yoreo JJ (2005) Modulation of calcium oxalate monohydrate crystallization by citrate through selective binding to atomic steps. *J Am Chem Soc* 127:9036–9044
52. Rez P, Sinha S, Gal A (2014) Nanocrystallite model for amorphous calcium carbonate. *J Appl Cryst* 47:1651–1657
53. Riese RJ, Riese JW, Kleinman JG, Wiessner JH, Mandel GS, Mandel NS (1988) Specificity in calcium oxalate adherence to papillary epithelial cells. *Am J Physiol* 255:F1025–F1032
54. Robertson WG, Peacock M, Nordin BEC (1971) Calcium oxalate crystalluria and urine saturation in recurrent renal stone-formers. *Clin Sci* 40:365–374
55. Rodgers AL (1983) Common ultrastructural features in human calculi. *Micron* 14:219–224
56. Rodgers AL, Cox TA, Noakes TD, Lombard CJ (1992) Crystalluria in marathon runners IV black subjects. *Urol Res* 20:27–33
57. Rodgers AL, Greyling KG, Irving RA, Noakes TD (1988) Crystalluria in marathon runners II ultra-marathon—males and females. *Urol Res* 16:89–93
58. Rodgers AL, Greyling KG, Noakes TD (1991) Crystalluria in marathon runners III stone-forming subjects. *Urol Res* 19:189–192
59. Ryall RL, Chauvet MC, Grover PK (2005) Intracrystalline proteins and urolithiasis: a comparison of the protein content and ultrastructure of urinary calcium oxalate monohydrate and dihydrate crystals. *BJU Int* 96:654–663
60. Ryall RL, Fleming DE, Doyle IR, Evans NA, Dean CJ, Marshall VR (2001) Intracrystalline proteins and the hidden ultrastructure of calcium oxalate urinary crystals: implications for kidney stone formation. *J Struct Biol* 134:5–14
61. Ryall RL, Fleming DE, Grover PK, Chauvet M, Dean CJ, Marshall VR (2000) The hole truth: Intracrystalline proteins and calcium oxalate kidney stones. *Mol Urol* 4:391–402
62. Ryall RL, Grover PK, Turgood LA, Chauvet MC, Fleming DE, van Bronswijk W (2007) The importance of a clean face: the effect of different washing procedures on the association of Tamm–Horsfall glycoprotein and other urinary proteins with calcium oxalate crystals. *Urol Res* 35:1–14
63. Sandersius S, Rez P (2007) Morphology of crystals in calcium oxalate kidney stones. *Urol Res* 35:287–293
64. Schubert G, Brien G (1981) Crystallographic investigations of urinary calcium oxalate calculi. *Int Urol Nephrol* 13:249–260
65. Schubert G, Brien G, Lenk S, Koch R (1983) Texture examinations on grain and thin section preparations of calcium oxalate calculi and their relations to pathogenetic parameters. *Urol Res* 11:111–115
66. Sheng X, Ward MD, Wesson JA (2003) Adhesion between molecules and calcium oxalate crystals: Critical interactions in kidney stone formation. *J Am Chem Soc* 125:2854–2855
67. Sheng XX, Jung TS, Wesson JA, Ward MD (2005) Adhesion at calcium oxalate crystal surfaces and the effect of urinary constituents. *Proc Natl Acad Sci* 102:267–272
68. Sours RE, Fink DA, Cox KA, Swift JA (2005) Uric acid dye inclusion crystals. *Mol Cryst Liq Cryst* 440:187
69. Spector M, Garden NM, Rous SN (1978) Ultrastructure and pathogenesis of human urinary calculi. *Br J Urol* 50:12–15
70. Stapleton AMF, Ryall RL (1995) Blood coagulation proteins and urolithiasis are linked: crystal matrix protein is the F1 activation peptide of human prothrombin. *Br J Urol* 75:712–719
71. Stapleton AMF, Simpson RJ, Ryall RL (1993) Crystal matrix protein is related to human prothrombin. *Biochem Biophys Res Commun* 195:1199–1203
72. Talham DR, Backov R, Benitez IO, Sharbaugh DM, Whipps S, Khan SR (2006) Role of lipids in urinary stones: studies of calcium oxalate precipitation at phospholipid langmuir monolayers. *Langmuir* 22:2450–2456
73. Tazzoli V, Domeneghetti C (1980) The crystal structures of whewellite and weddellite: re-examination and comparison. *Am Mineral* 65:327–334
74. Thomas A, Rosseeva E, Hochrein O, Carrillo-Cabrera W, Simon P, Duchstein P, Zahn D, Kniep R (2012) Mimicking the growth of a pathologic biomineral: shape development and structures of calcium oxalate dihydrate in the presence of polyacrylic acid. *Chem—A Eur J* 18:4000–4009
75. Werness PG, Bergert JH, Smith LH (1981) Crystalluria. *J Cryst Growth* 53:166–181
76. Werness PG, Duckworth SC, Smith LH (1979) Calcium oxalate dihydrate crystal growth. *Investig Urol* 17:230–233
77. Wesson JA, Ward MD (2007) Pathological biomineralization of kidney stones. *Elements* 3:415–421
78. Whipps S, Khan SR, Palko FJ, Backov R, Talham DR (1998) Growth of calcium oxalate monohydrate at phospholipid Langmuir monolayers. *J Cryst Growth* 192:243–249
79. Wulff G (1901) On the question of speed of growth and dissolution of crystal surfaces. *Z Kristallogr und Mineral* 34:449–530